

Twisted Aspirin Crystals

Xiaoyan Cui,[†] Andrew L. Rohl,[‡] Alexander Shtukenberg,^{*,†} and Bart Kahr^{*,†}

[†]Department of Chemistry, New York University, 100 Washington Square East, Silver Center, Room 1001, New York, New York 10003, United States

[‡]Department of Chemistry, Curtin University, P.O. Box U1987, Perth, Western Australia 6845, Australia

ABSTRACT: Banded spherulites of aspirin have been crystallized from the melt in the presence of salicylic acid either generated from aspirin decomposition or added deliberately (2.6–35.9 mol %). Scanning electron microscopy, X-ray diffraction analysis, and optical polarimetry show that the spherulites are composed of helicoidal crystallites twisted along the $\langle 010 \rangle$ growth directions. Mueller matrix imaging reveals radial oscillations in not only linear birefringence, but also circular birefringence, whose origin is explained through slight ($\sim 1.3^\circ$) but systematic splaying of individual lamellae in the film. Strain associated with the replacement of aspirin molecules by salicylic acid molecules in the crystal structure is computed to be large enough to work as the driving force for the twisting of crystallites.

Most chemists in training have synthesized and crystallized aspirin; $\sim 45\,000$ tons are manufactured and consumed annually. That said, it seems unlikely that the crystallization of aspirin will continue to surprise, but that is precisely what transpired with the discovery of a new polymorph in 2005,¹ precipitated by the computational predictions of new crystalline forms.² This work sparked a wave of new research into aspirin crystallization from solution.^{3–6}

What of crystallization from the melt or the glassy state ($T_g = 243\text{ K}$)? Researchers have investigated amorphous aspirin of late but do not comment on how these preparations ultimately crystallize.^{7–14} Here, we aim to illustrate that aspirin crystals grow from the melt as helicoidal ribbons with pitches that vary from about $20\ \mu\text{m}$ to larger than $1\ \text{mm}$ depending on the growth conditions. The possibility of this unusual growth mode is suggested by the appearance of aspirin as the 90th entry in a table of 135 organic compounds in a rare book about *Twisted Crystals*.¹⁵ The most authoritative source on the crystallization of pharmaceuticals from the melt¹⁶ gives no hint whatsoever that aspirin might be of interest to those interested in nonclassical crystal growth mechanisms or pattern formation in nature.

Crystalline aspirin (2–4 mg) powder (Sigma 99%, mp = $133.5\text{ }^\circ\text{C}$) was melted between a glass slide and a coverslip. Banded spherulites form at temperatures $<25\text{ }^\circ\text{C}$ at a rate of about $0.02\ \text{mm/min}$. At higher temperatures, spherulites are irregular and bands become indistinct. Fibrils grow radially from a central nucleus and display concentric rings of varying linear retardance (Figure 1). The spherulites are optically positive; the larger refractive index is directed along the radii.

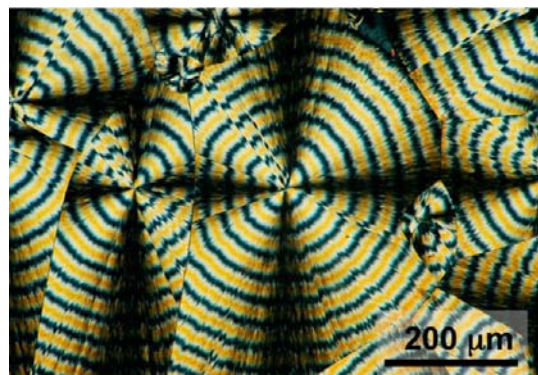


Figure 1. Aspirin (salicylic acid concentration in the melt is 19 mol %) spherulites grown at $4\text{ }^\circ\text{C}$.

We have established previously that impurities are likely to be a necessary precondition for twisting.^{17–19} As such, we surmised that the hydrolytic decomposition product of aspirin that forms on melting, salicylic acid, was the agent that actualized the optical oscillations through twisting. In fact, the most effective way to grow banded aspirin spherulites is to mix 19 mol % salicylic acid (Mallinckrodt 99%, mp = $158\text{ }^\circ\text{C}$) with aspirin prior to melting. Films grown in this way were approximately $2\ \mu\text{m}$ thick with a pitch of about $100\ \mu\text{m}$. Band spacing (pitch) decreases from ~ 800 to $20\ \mu\text{m}$ as the concentration of salicylic acid in the melt increases from 2.6 to 35.9 mol % (Figure 2). Nominally, pure aspirin spherulites are characterized by larger pitch of 1–2 mm. In this case, banding can arise from traces of salicylic acid formed during melting.

The banded spherulites grew as either of the two known polymorphs of aspirin or as a mixture of the two; it is difficult to distinguish them by powder X-ray diffraction as they are very close in structure (monoclinic, $P2_1/c$) and frequently intergrown.^{3,4,14} Crystal data, Form I²⁰ (II)¹: $a = 11.242(7)\ \text{\AA}$ ($12.095(7)\ \text{\AA}$), $b = 6.539(4)\ \text{\AA}$ ($6.491(4)\ \text{\AA}$), $c = 11.245(9)\ \text{\AA}$ ($11.323(6)\ \text{\AA}$), $\beta = 95.90(1)^\circ$ ($111.509(9)^\circ$). The previously measured optical properties of aspirin single crystals are most likely a good approximation or average of Forms I and/or II: $n_x = 1.5066$, $n_y = 1.6464$, and $n_z = 1.6604$ at $546\ \text{nm}$.²¹ n_z and the optical plane are normal to (010) . n_x and n_y are nearly bisected by $[001]$.^{21–25}

The excess salicylic acid in the banded spherulites was sublimed by heating the films at $70\text{ }^\circ\text{C}$ for 100 min without significant loss of aspirin.²⁶ The samples were coated with an evaporated gold layer (3–6 nm) thick and imaged by scanning

Received: January 24, 2013

Published: February 20, 2013

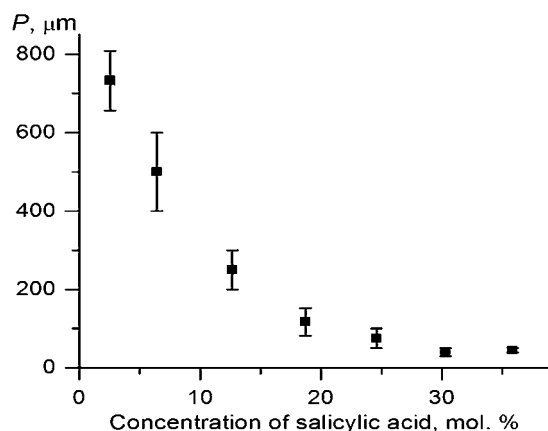


Figure 2. Pitch, P , as a function of salicylic acid concentration in the melt from which the spherulites grew, $T = 20\text{ }^{\circ}\text{C}$.

electron microscopy (SEM). The spherulites comprised ribbon-shaped or lamellar crystallites approximately $2\text{--}5\text{ }\mu\text{m}$ in width and $100\text{--}250\text{ nm}$ in thickness twisted along the growth direction (Figure 3). The optical bands represent a periodic

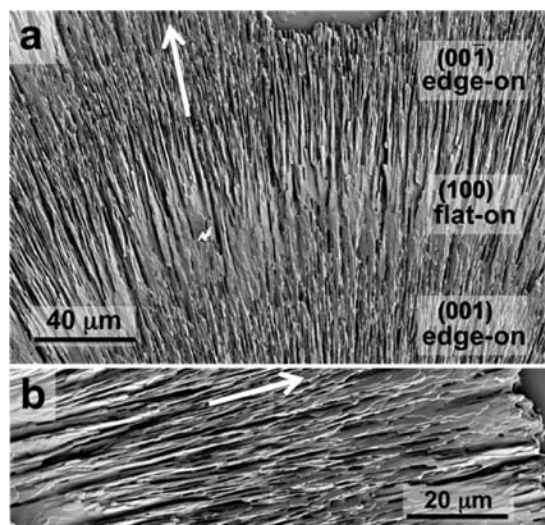


Figure 3. SEM images of aspirin spherulites (salicylic acid concentration in the melt 19 mol %; $T = 20\text{ }^{\circ}\text{C}$) showing overall arrangement of lamellae in the spherulite (a) and details of twisting (b). Growth direction is shown by arrows.

change in the orientation of crystallites from edge-on to flat-on to edge-on again. X-ray diffraction examination showed that the large faces correspond to $\{100\}$ planes. Knowing that the larger refractive index is always directed along the spherulite radius and taking into account the orientation of the optical indicatrix with respect to crystallographic axes, the growth direction of crystallites was shown to be $\langle 010 \rangle$. Thus, the birefringence in banded aspirin spherulites should oscillate between $n_z - n_y = 0.014$ and $n_z - n_x = 0.154$ (at 546 nm).

Mueller matrix imaging polarimetry^{19,27,28} was used to analyze the linear birefringence ($\text{LB} = 2\pi(n_{0^\circ} - n_{90^\circ})L/\lambda$, where L is the thickness, λ is the wavelength, and n_{0° and n_{90° are the refractive indices for orthogonal polarizations) and circular birefringence ($\text{CB} = 2\pi(n_L - n_R)L/\lambda$, where n_L and n_R are refractive indices for left and right circularly polarized light) of aspirin spherulites. Figure 4 shows the $|\text{LB}|$ and CB micrographs ($\lambda = 532\text{ nm}$) derived from the raw Mueller

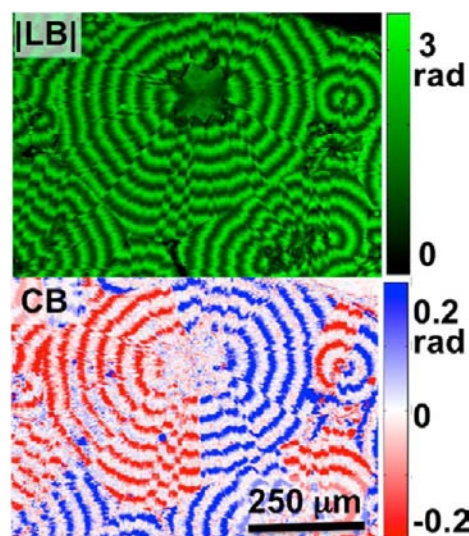


Figure 4. $|\text{LB}|$ and CB micrographs ($\lambda = 532\text{ nm}$) of aspirin spherulites (salicylic acid concentration in the melt 19 mol %; $T = 20\text{ }^{\circ}\text{C}$).

matrix.²⁹ (LB and CB are standard abbreviations used in Mueller matrix polarimetry, but the quantities displayed are thickness dependent and are more properly described as $|\text{LRI}|$ and CR for 'retardances'. We nevertheless adhere to standard nomenclature.) The $|\text{LB}|$ oscillates along the growth direction as was evident from the simple inspection between crossed polarizers (Figure 1). The CB micrograph is more interesting. It shows that CB is non-zero even though aspirin is centrosymmetric and cannot have natural optical activity. The etiology of the sensitivity to circularly polarized light must lie elsewhere. Moreover, each spherulite is bisected into halves that are, respectively, dextrorotatory and levorotatory. The CB oscillates smoothly from zero to a positive or negative value in each half, and it is in phase with the LB (Figures 4 and 5).

Superimposition of Mueller matrix and SEM images (Figure 5) shows that regions with primarily positive and negative CB correspond to the opposite $\langle 010 \rangle$ growth directions of aspirin crystallites. Because of the monoclinic $2/m$ symmetry, twisting of the aspirin crystallite is right-handed for one $\langle 010 \rangle$ direction and left-handed for the opposite direction. Since strong CB takes place only when edge-on lamellae change orientation to flat-on, right-handed helicoids show positive CB whereas left-handed helicoids give negative CB.

We recently reported concentric CB oscillations in mannitol banded spherulites¹⁹ that resulted from splaying of overlapped, anisotropic lamellae, a picture consistent with the very first model of artificial optical activity, Reusch's pile of misoriented mica plates.^{30,31} Reusch claimed that he could mimic optical rotation in a crystal by stacking flakes of mica each rotating in the same sense by a small amount from layer to layer. This model can be applied to aspirin by modeling the optical properties of the polycrystalline films.

To model LB, a refractive index ellipsoid was smoothly rotated around n_z , so that π rotation corresponded to the observed pitch (Figure 5). The thickness of the sample, $1.6\text{ }\mu\text{m}$, was measured by atomic force microscopy (AFM). Observed and simulated birefringence oscillates likewise. The near perfect fit was obtained for refractive indices (Figure 5) of $n_x = 1.53$, $n_y = 1.63$ and $n_z = 1.66$.

CB was modeled assuming that the $1.6\text{ }\mu\text{m}$ thick film was composed of 150 nm thick ribbons. The linear retardance of

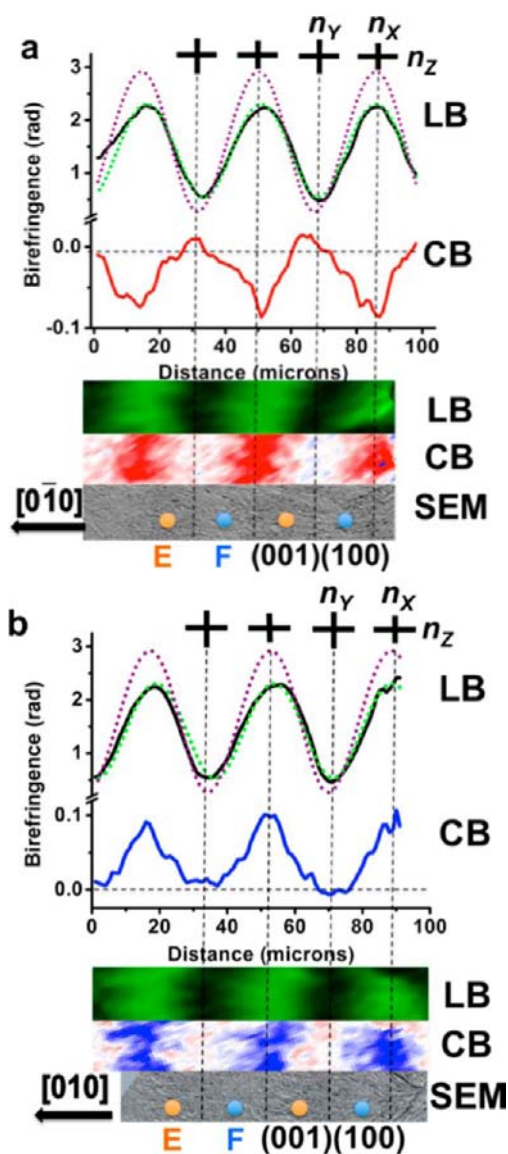


Figure 5. (a and b) Hemispheres of an aspirin spherulite (salicylic acid concentration in the melt 19 mol %; $T = 20\text{ }^{\circ}\text{C}$). Optical data measured at 532 nm. From top to bottom: plus signs indicate the orientation of principal refractive indices, linear birefringence (LBI) as solid black line extracted from Mueller matrix micrographs, green dotted line is the simulated LBI with best fit refractive indices (n_x , n_y , n_z), purple dotted line is simulated LBI with real thickness and refractive indices based on single crystal measurements, circular birefringence (CB) extracted from Mueller matrix micrograph, extracts of LBI and CB micrographs, sections of SEM micrographs of the corresponding areas. Blue and orange dots and letters (F,E) indicate flat-on and edge-on orientations, respectively. Arrows indicate the growth directions.

each layer was taken as $1/10$ (0.22 rad) of the maximum measured linear retardance (2.2 rad) (Figure 5). The Mueller matrix representing an ensemble of splayed ribbons was calculated by multiplying a typical Mueller matrix for a retarder, by nine others progressively rotated in the same sense. The maximum measured circular retardance was fitted assuming a mutual layer misorientation of about $\sim 1.3^{\circ}$ (clockwise looking at the light source for negative CB, and of course, counter-clockwise for positive CB) for the data shown in Figure 5. Misoriented lamellae and strong CB are found in the transition

regions between flat-on and edge-on orientations.¹⁹ However, unlike mannitol,¹⁹ here CB is strong for only edge-on \rightarrow flat-on domains and not flat-on \rightarrow edge-on domains. The reason for the difference is not clear in this case. But, there is not reason by symmetry that the splay on the leading and trailing side of an edge-on band must be the same.

The fraction of salicylic acid in the aspirin crystallites was monitored by thermogravimetric analysis at $75\text{ }^{\circ}\text{C}$. Salicylic acid is much more volatile than aspirin. The salicylic acid that could not be sublimed at this temperature was presumably trapped in aspirin crystals. The trapped fraction was about half of the salicylic acid added to the mixture: 1.2 and 15.0 mol % did not sublime when 2.6 and 30.3 mol % were admixed in the melt, respectively.

We had earlier surmised that additive-induced twisting of molecular crystals was likely a consequence of stress associated with mixed crystal growth.^{17–19} Therefore, it was incumbent upon us to estimate how much strain is required to twist an aspirin ribbon of the dimensions that we observed.

Deformation of the aspirin unit cell by incorporation of salicylic acid was calculated using the COMPASS force field³² as embodied in the Materials Studio program suite (Accelrys). This force field has been shown to reproduce the elastic properties of aspirin well³³ and is thus suited to the strain calculations reported here. Salicylic acid molecules were docked in place of aspirin molecules in supercells of increasing size so as to vary the guest over the concentration range 0.5–12.5 mol %. Strain tensors were calculated by comparing the unit cell dimensions of optimized mixed crystal structures with the unit cell of pure aspirin likewise optimized (Figure 6).

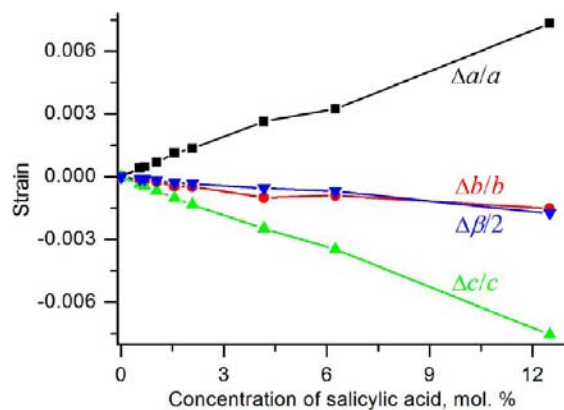


Figure 6. Calculated components of the strain tensor of the aspirin crystal related to incorporation of salicylic acid into the crystal lattice.

We can estimate the required minimum lattice strain to twist aspirin crystals using a procedure developed earlier.³⁴ The elastic energy required to twist a circular rod of radius r is given as:

$$U = \frac{\pi^3 G r^4 H}{4P^2} = \frac{\pi^2 G r^2 V}{4P^2} \quad (1)$$

where G is the shear modulus, H is the length of the rod, and V is its volume. The dependence of elastic energy on the radius is more complex for crystals with polyhedral cross sections, but the difference is typically a constant factor close to unity.

The elastic energy (U) can result from mismatch strain between different subvolumes of the crystal. Accurate calculation of the strain requires information on the spatial

distribution of lattice constants over the cross section. This information is not available. However, the *lower* estimate of the required strain can be obtained using a bimetallic strip model. The elastic energy of a bimetallic strip is equal to

$$U = \frac{\varepsilon^2 EV}{2} \cdot \frac{h_1 h_2}{(h_1 + h_2)^2} \quad (2)$$

where E is Young's modulus, h_1 and h_2 are thicknesses of the strips, and ε is the misfit strain between these parts. The highest energy corresponds to $h_1 = h_2$. Assuming that all this deformation is redistributed to induce a twist moment in the rod of the same volume, eqs 1 and 2 can be combined to give $\varepsilon = \pi r/P$ ($G \approx E/2$).

For the sample containing ~ 8 mol % of salicylic acid in the crystal (19 mol % in the melt), the thickness of the crystallites is 200 nm ($= 2r$) and the pitch is 120 μm (Figure 3) which gives $\varepsilon = 2.6 \times 10^{-3}$. This degree of strain can be reached by subvolumes having a difference of 2 mol % of salicylic acid (Figure 6). At least this difference in composition—domains with 7 and 9 mol % of salicylic acid from the melt—is chemically quite reasonable.

In summary, the growth-induced twisting of aspirin crystallites grown from the melt is driven by salicylic acid during mixed crystal formation. The nonclassical morphology of the most popular of all pharmaceuticals underscores the common yet overlooked distortions of crystals into non-polyhedral shapes that accompany high driving forces in the presence of appropriate additives. The individual aspirin crystals assemble as spherulites that display optical activity on the mesoscale that is a consequence of the organization of helicoidal crystalline ribbons, locally, and globally; each spherulite divides into heterochiral halves. The determination of the absolute sense of crystal growth in enantiopolar directions and the determination of the salicylic acid concentration variance in submicrometer sized crystallites remain future experimental challenges.

EXPERIMENTAL

Optical micrographs in Figures 4 and 5 were made with a home-built Mueller matrix imaging polarimeter with mechanical light modulation. This instrument was described previously.^{19,34} Scanning electron micrographs were recorded with a MERLIN field-emission scanning electron microscope (Carl Zeiss) using a standard Everhart-Thornley type detector at an acceleration voltage of 1–2.5 kV. Thickness of the sample and each lamella were measured by atomic force microscope (MFP-3D-SA System, Asylum Research). Thermogravimetric analyses were made with a Perkin-Elmer Pyris 1 instrument.

AUTHOR INFORMATION

Corresponding Author

bart.kahr@nyu.edu; shtukenberg@mail.ru

Notes

The authors declare no competing financial interest.

ACKNOWLEDGMENTS

B.K. thanks the NSF (CHE-0845526, DMR-1105000) for support of this research. The authors acknowledge the NSF CRIF Program (CHE-0840277) and the NSF MRSEC Program (DMR-0820341) for the Bruker AXS D8 DISCOVER GADDS Microdiffractometer. The scanning electron microscope was purchased with financial support from the MRI

program of the NSF under Award DMR-0923251. The authors are grateful for the assistance of Dr. J. H. Freudenthal and Ms. Haley Smith, and thank Professor M. D. Ward for the use of his AFM.

REFERENCES

- (1) Vishweshwar, P.; McMahon, J. A.; Oliveira, M.; Peterson, M. L.; Zaworotko, M. J. *J. Am. Chem. Soc.* **2005**, *127*, 16802.
- (2) Ouvrard, C.; Price, S. L. *Cryst. Growth Des.* **2004**, *4*, 1119.
- (3) Bond, A. D.; Boese, R.; Desiraju, G. R. *Angew. Chem., Int. Ed.* **2007**, *46*, 615.
- (4) Bond, A. D.; Boese, R.; Desiraju, G. R. *Angew. Chem., Int. Ed.* **2007**, *46*, 618.
- (5) Heng, J. Y. Y.; Bismarck, A.; Lee, A. F.; Wilson, K.; Williams, D. R. *J. Pharm. Sci.* **2007**, *96*, 2134.
- (6) Koleva, B. B. *J. Mol. Struct.* **2006**, *800*, 23.
- (7) Nath, R.; El Goresy, T.; Geil, B.; Zimmermann, H.; Bohmer, R. *Phys. Rev. E* **2006**, *74*, 021506.
- (8) Duddu, S. P.; Weller, K. J. *J. Pharm. Sci.* **1996**, *85*, 345.
- (9) Fukuoka, E.; Makita, M.; Nakamura, Y. *Chem. Pharm. Bull.* **1991**, *39*, 2087.
- (10) Johari, G. P.; Kim, S.; Shanker, R. M. *J. Pharm. Sci.* **2007**, *96*, 1159.
- (11) Ko, J. H.; Kim, T. H.; Lee, K. S.; Kojima, S. *J. Non-Cryst. Solids* **2011**, *357*, 547.
- (12) Nath, R.; Nowaczyk, A.; Geil, B.; Bohmer, R. *J. Non-Cryst. Solids* **2007**, *353*, 3788.
- (13) Zhang, Y.; Tyagi, M.; Mamontov, E.; Chen, S. H. *J. Phys.: Condens. Matter* **2012**, *24*, 064112.
- (14) Wen, S.; Beran, G. J. O. *Cryst. Growth Des.* **2012**, *12*, 2169.
- (15) Bernauer, F. "Gedrilte" Kristalle; Gebrüder Borntraeger: Berlin, 1929.
- (16) Kuhnert-Brandstätter, M. *Thermomicroscopy in the Analysis of Pharmaceuticals*; Pergamon Press: Oxford, 1971.
- (17) Shtukenberg, A.; Gunn, E.; Gazzano, M.; Freudenthal, J.; Camp, E.; Sours, R.; Rosseeva, E.; Kahr, B. *ChemPhysChem* **2011**, *12*, 1558.
- (18) Kahr, B.; Shtukenberg, A.; Gunn, E.; Carter, D. L.; Rohl, A. L. *Cryst. Growth Des.* **2011**, *11*, 2070.
- (19) Shtukenberg, A. G.; Cui, X.; Freudenthal, J.; Gunn, E.; Camp, E.; Kahr, B. *J. Am. Chem. Soc.* **2012**, *134*, 6354.
- (20) Aubrey-Medendorp, C.; Parkin, S.; Li, T. *J. Pharm. Sci.* **2008**, *97*, 1361.
- (21) Niini, V. R. Z. *Kristallogr.* **1931**, *79*, 532.
- (22) Hayman, J. L.; Wagener, L. R.; Holden, E. F. *J. Am. Pharm. Assoc.* **1925**, *14*, 388.
- (23) Nitta, I.; Watanabé, T. *Sci. Pap. Inst. Phys. Chem. Res.* **1937**, *31*, 125.
- (24) Watanabé, S.; Watanabé, A. *Proc. Imp. Acad. (Tokyo)* **1935**, *11*, 379.
- (25) Winchell, A. N. *The Optical Properties of Organic Compounds*; McCrone Research Institute: Chicago, IL, 1987.
- (26) Gore, A. Y.; Naik, K. B.; Kildsig, D. O.; Peck, G. E.; Smolen, V. F.; Banker, G. S. *J. Pharm. Sci.* **1968**, *57*, 1850.
- (27) Freudenthal, J. H.; Hollis, E.; Kahr, B. *Chirality* **2009**, *21*, E20.
- (28) Ye, H.-M.; Xu, J.; Freudenthal, J.; Kahr, B. *J. Am. Chem. Soc.* **2011**, *133*, 13848.
- (29) Arteaga, O.; Canillas, A. *J. Opt. Soc. Am. A* **2009**, *26*, 783.
- (30) Reusch, E. *Ann. Phys. Chem.* **1869**, *138*, 628.
- (31) Joly, G.; Billard, J. *J. Opt.* **1981**, *12*, 323.
- (32) Sun, H. *J. Phys. Chem. B* **1998**, *102*, 7338.
- (33) Bauer, J. D.; Haussühl, E.; Winkler, B.; Arbeck, D.; Milman, V.; Robertson, S. *Cryst. Growth Des.* **2010**, *10*, 3132.
- (34) Shtukenberg, A. G.; Freudenthal, J.; Kahr, B. *J. Am. Chem. Soc.* **2010**, *132*, 9341.